



Numerical Simulations of Two Components Ecological Models with Sinc Collocation Method

Ali Barati * and Ali Atabaigi

ABSTRACT: It is well known that reaction-diffusion systems can describe the interactions of different species in ecological systems. In this work, we propose a numerical method for solving a general two-species reaction-diffusion system. The method comprises a standard finite difference to discretize in time direction and Sinc collocation method in spatial direction. A series of numerical experiments demonstrate the accuracy and good performance of the algorithm. The biological significance of the numerical results was also discussed and plotted in figures.

Key Words: Reaction-diffusion systems, predator-prey, Sinc collocation method.

Contents

1 Introduction	147
2 Notation and background	149
3 Description of method	152
4 Numerical results	156
5 Conclusions	162

1. Introduction

Reaction-diffusion equations may be used to model many natural phenomena and practical problems which arise from a variety of disciplines such as physics, chemistry, medicine and so on. These equations are a useful tool for modeling the spatiotemporal dynamics of populations in ecology [1,2]. The study of reaction-diffusion problems in ecological context have gained a huge amount of scientific interest, due to their practical relevance and emergence of some interesting phenomena such as spatial patterns, oscillating solutions, phase planes and multiple steady states to mention a few.

In recent years, there have been considerable interests in spatial and temporal behavior of interacting species in ecosystems. Pattern formation study in reaction-diffusion systems is a very active research area. Since Turing [3] first proposed reaction-diffusion theory to describe the range of spatial patterns observed in the

* Corresponding author
2010 *Mathematics Subject Classification*: 65M22, 65N30, 35F20.
Submitted August 01, 2017. Published January 17, 2018

developing embryo, reaction-diffusion systems have been studied extensively to explain patterns in fish skin, mammalian coat markings, phyllotaxis, predator-prey systems, terrestrial vegetation, plankton, intertidal communities and so on (see Ref. [5,6,7,8,9]).

Predator-prey model is one of the most important population dynamical models. There are many factors which affect population dynamics in predator-prey models. One crucial component of predator-prey relationships is predator-prey interaction (also called functional response), which can be classified in to many different types, such as Holling I-IV types, Hassell-Varley type, Beddington-DeAngelis type, Crowley-Martin type, and etc.

Predator-prey systems have been studied by many researchers in various forms. For instance, in bacteria ecology, computer simulations of complex spatiotemporal patterns [10,11] of *Bacillus subtilis* based on deterministic models [12], Allee effect of patchy invasion on predator-prey dynamics [13]. Jiang et al. in [14] consider a predator-prey model with Beddington-DeAngelis functional response subject to the homogeneous Neumann boundary condition. Moreover, Wang et al. [15] investigated the spatial pattern formation of a predator-prey system with prey-dependent functional response of Ivlev type and reaction-diffusion whereas the analysis of predator-prey systems showing the Holling type II functional response is examined in Garvie and Trenchea [16]. Moreover, we can point to other efficient numerical methods for solving the reaction-diffusion equations arising in biology such as [17,18,19,20,21].

In this paper, we consider the following general two-species reaction-diffusion system

$$\begin{cases} \frac{\partial u}{\partial t} = d_u \frac{\partial^2 u}{\partial x^2} + f(u, v), & (x, t) \in \Omega \times (0, \infty), \\ \frac{\partial v}{\partial t} = d_v \frac{\partial^2 v}{\partial x^2} + g(u, v), & (x, t) \in \Omega \times (0, \infty), \end{cases} \quad (1.1)$$

subject to the initial conditions:

$$u(x, 0) = u_0(x), \quad v(x, 0) = v_0(x) \quad x \in \bar{\Omega}, \quad (1.2)$$

and zero-flux boundary conditions

$$\frac{\partial u}{\partial \nu} = \frac{\partial v}{\partial \nu} = 0, \quad (x, t) \in \partial\Omega \times (0, \infty), \quad (1.3)$$

where $u(x, t)$ and $v(x, t)$ represent the species densities, Ω is a bounded region with the smooth boundary $\partial\Omega$ in \mathbb{R} (here we assume $\Omega = (a, b)$), ν is the outward unit normal vector on $\partial\Omega$. The positive constants d_u and d_v are the diffusion coefficients corresponding to u and v , also f and g are reaction kinetics.

The homogeneous Neumann boundary condition means that model (1.1) is self-contained and has no population flux across the boundary $\partial\Omega$.

We assume that the point (u_s, v_s) is a positive equilibrium point of the homogeneous system

$$\frac{du}{dt} = f(u, v), \quad \frac{dv}{dt} = g(u, v), \quad (1.4)$$

that is $f(u_s, v_s) = 0, \quad g(u_s, v_s) = 0$

In [3], Turing concluded that the reaction-diffusion model (1.1) may exhibit spatial patterns under the following two conditions: the equilibrium (u_s, v_s) is linearly stable in the absence of diffusion; and the equilibrium becomes linearly unstable in the presence of diffusion. Such an instability is called a *Turing instability* or *diffusion-driven instability*.

In this paper, a numerical method applied for solving couple system (1.1) which is based on Sinc basis functions. Sinc methods have been studied extensively and found to be a very effective technique, particularly for problems with singular solutions and those on unbounded domain. In addition, Sinc function seems that be useful for problems that their solutions have oscillatory behavior in domain. Sinc method originally introduced by Stenger [22] which is based on the Whittaker-Shannon-Kotel'nikov sampling theorem for entire functions. The books [23] and [24] provide excellent overviews of the existing Sinc methods for solving ODEs and PDEs.

In recent years, a lot of attentions have been devoted to the study of the Sinc method to investigate various scientific models. The efficiency of the Sinc method has been formally proved by many researchers Bialecki [25], Rashidinia et al. [26, 27], EL-Gamel [28], Okayama et al. [29] and Saadatmandi and Dehghan [30]. The paper is organized as follows. In section 2, we review some basic facts about the Sinc approximation. In section 3, we discretized the reaction-diffusion system in temporal variable by means of implicit Euler method and then we applied the Sinc-collocation method for solving of the arising system of nonlinear ordinary differential equations in each time level. Some numerical examples will be presented in section 4, and at the end we conclude implementation, application and efficiency of the proposed scheme.

2. Notation and background

The goal of this section is to recall notations and definitions of the Sinc function and state some known theorems that are important for this paper.

The Sinc function is defined on $-\infty < x < \infty$ by

$$Sinc(x) = \begin{cases} \frac{\sin(\pi x)}{\pi x}, & x \neq 0, \\ 1, & x = 0. \end{cases}$$

For $h > 0$ we will denote the Sinc basis functions by

$$S(k, h)(x) = sinc\left(\frac{x - kh}{h}\right), \quad k = 0, \pm 1, \pm 2, \dots$$

let f be a function defined on \mathbb{R} then for $h > 0$ the series

$$C(f, h)(x) = \sum_{k=-\infty}^{\infty} f(kh)S(k, h)(x),$$

is called the Whittaker cardinal expansion of f whenever this series converges. The properties of Whittaker cardinal expansions have been studied and are thoroughly

surveyed in Stenger [24]. These properties are derived in the infinite strip D_d of the complex plane where $d > 0$

$$D_d = \{\zeta = \xi + i\eta : |\eta| < d \leq \frac{\pi}{2}\}.$$

Approximations can be constructed for infinite, semi-finite, and finite intervals. To construct approximation on the interval (a, b) , we consider the conformal map

$$\phi(z) = \ln\left(\frac{z-a}{z-b}\right), \quad (2.1)$$

which maps the eye-shaped region

$$D_E = \{z = x + iy; |\arg(\frac{z-a}{z-b})| < d \leq \frac{\pi}{2}\},$$

onto the infinite strip D_d .

For the Sinc method, the basis functions on the interval (a, b) for $z \in D_E$ are derived from the composite translated Sinc function:

$$S_k(z) = S(k, h) \circ \phi(z) = \text{sinc}\left(\frac{\phi(z) - kh}{h}\right). \quad (2.2)$$

The function

$$z = \phi^{-1}(\omega) = \frac{a + be^\omega}{1 + e^\omega},$$

is an inverse mapping of $\omega = \phi(z)$. We define the range of ϕ^{-1} on the real line as

$$\Gamma = \{\psi(u) = \phi^{-1}(u) \in D_E : -\infty < u < \infty\} = (a, b).$$

The sinc grid points $z_j \in (a, b)$ in D_E will be denoted by x_j because they are real. For the evenly spaced nodes $\{jh\}_{j=-\infty}^{\infty}$ on the real line, the image which corresponds to these nodes is denoted by

$$x_j = \phi^{-1}(jh) = \frac{a + be^{jh}}{1 + e^{jh}}, \quad j = 0, \pm 1, \pm 2, \dots \quad (2.3)$$

Definition 2.1. Let $B(D_E)$ is the class of functions f which are analytic in D_E such that

$$\int_{\psi(u+\Sigma)} |f(z)| dz \rightarrow 0, \quad \text{as } u \rightarrow \pm\infty \quad (2.4)$$

where $\Sigma = \{i\eta : |\eta| < d \leq \frac{\pi}{2}\}$ and satisfy

$$N(f) \equiv \int_{\partial D_E} |f(z)| dz < \infty, \quad (2.5)$$

where ∂D_E represents the boundary of D_E .

Definition 2.2. Let $L_\alpha(D_E)$ be the set of all analytic function u in D_E , for which there exists a constant C such that

$$|u(z)| \leq C \frac{|\rho(z)|^\alpha}{[1 + |\rho(z)|]^{2\alpha}}, \quad z \in D_E, \quad 0 < \alpha \leq 1. \quad (2.6)$$

where $\rho(z) = e^{\phi(z)}$.

Theorem 2.3. (Stenger [24]) If $\phi' u \in B(D_E)$, and let

$$\sup_{-\frac{\pi}{h} \leq t \leq \frac{\pi}{h}} \left| \left(\frac{d}{dx} \right)^l e^{it\phi(x)} \right| \leq C_1 h^{-l}, \quad x \in \Gamma,$$

for $l = 0, 1, \dots, m$ with C_1 a constant depending only on m and ϕ . If $u \in L_\alpha(D_E)$ then taking $h = \sqrt{\pi d / \alpha N}$ it follows that

$$\sup_{x \in \Gamma} \left| u^{(l)}(x) - \left(\frac{d}{dx} \right)^l \sum_{k=-N}^N u(x_k) S_k(x) \right| \leq C N^{(l+1)/2} \exp(-(\pi d \alpha N)^{1/2}),$$

where C is a constant depending only on u, d, m, ϕ and α .

The Sinc-collocation method requires that the derivatives of composite Sinc function be evaluated at the nodes. We need to recall the following lemma.

Lemma 2.4. (Lund and Bowers [23]) Let ϕ be the conformal one-to-one mapping of the simply connected domain D_E onto D_d , given by (2.2). Then

$$\delta_{kj}^{(0)} = [S(k, h) \circ \phi(x)]|_{x=x_j} = \begin{cases} 1, & k = j, \\ 0, & k \neq j, \end{cases} \quad (2.7)$$

$$\delta_{kj}^{(1)} = h \frac{d}{d\phi} [S(k, h) \circ \phi(x)]|_{x=x_j} = \begin{cases} 0, & k = j, \\ \frac{(-1)^{(j-k)}}{j-k}, & k \neq j, \end{cases} \quad (2.8)$$

$$\delta_{kj}^{(2)} = h^2 \frac{d^2}{d\phi^2} [S(k, h) \circ \phi(x)]|_{x=x_j} = \begin{cases} \frac{-\pi^2}{3}, & k = j, \\ \frac{-2(-1)^{(j-k)}}{(j-k)^2}, & k \neq j, \end{cases} \quad (2.9)$$

in relations (2.7-2.9) h is step size and x_j is sinc grid given by (2.3).

It is convenient to define the following matrices:

$$\mathbf{I}^{(l)} = [\delta_{kj}^{(l)}], \quad l = 0, 1, 2, \quad (2.10)$$

where $\delta_{kj}^{(l)}$ denotes the (k, j) th element of the matrix $\mathbf{I}^{(l)}$. Note that the matrix $\mathbf{I}^{(2)}$ and $\mathbf{I}^{(1)}$ are symmetric and skew-symmetric matrices respectively, also $\mathbf{I}^{(0)}$ is identity matrix.

3. Description of method

First, we discretize reaction-diffusion system (1.1) in time direction by means of the implicit Euler method with uniform step size Δt as

$$u_t = \frac{u^{n+1} - u^n}{\Delta t}, \quad v_t = \frac{v^{n+1} - v^n}{\Delta t},$$

where $u^n = u(x, t_n)$, $u^0 = u(x, 0)$, $v^n = v(x, t_n)$, $v^0 = v(x, 0)$ and $t_n = n\Delta t$, $n = 1, 2, \dots$,

to get the following system of nonlinear ordinary differential equations:

$$\begin{cases} \frac{u^{n+1} - u^n}{\Delta t} = d_u D^2 u^{n+1} + f(u^{n+1}, v^{n+1}), \\ \frac{v^{n+1} - v^n}{\Delta t} = d_v D^2 v^{n+1} + g(u^{n+1}, v^{n+1}), \end{cases} \quad (3.1)$$

where $u^{n+1} = u(x, t_{n+1})$ and $v^{n+1} = v(x, t_{n+1})$ are the solutions of Eqs.(3.1) at $(n+1)$ th time level and $D = \frac{d}{dx}$.

Now we can rewrite equation (3.1) in the following form

$$\begin{cases} d_u D^2 \hat{u} + f(\hat{u}, \hat{v}) - \frac{1}{\Delta t} \hat{u} = -\frac{u^n}{\Delta t}, \\ d_v D^2 \hat{v} + g(\hat{u}, \hat{v}) - \frac{1}{\Delta t} \hat{v} = -\frac{v^n}{\Delta t}, \end{cases} \quad (3.2)$$

where $\hat{u} = u^{n+1}$, $\hat{v} = v^{n+1}$ and associated with homogeneous Neumann boundary conditions:

$$\hat{u}'(x) = \hat{v}'(x) = 0, \quad x \in \partial\Omega. \quad (3.3)$$

Then, we apply the Sinc-collocation method for solution of the system of equation (3.2) with given boundary conditions.

Since the Sinc basis functions in (2.2) do not have a derivative at endpoints a and b , and because the Neumann boundary conditions (3.3) must be handled at a and b by approximate solutions, Thus the approximate solutions for $\hat{u}(x)$ and $\hat{v}(x)$ in Eqs(3.2) are represented by formula

$$\begin{cases} \hat{u}(x) \approx \hat{u}_m(x) = c_{-N-1} w_a(x) + \sum_{k=-N}^N c_k \xi(x) S_k(x) + c_{N+1} w_b(x), \\ \hat{v}(x) \approx \hat{v}_m(x) = \rho_{-N-1} w_a(x) + \sum_{k=-N}^N \rho_k \xi(x) S_k(x) + \rho_{N+1} w_b(x), \end{cases} \quad (3.4)$$

$$m = 2N + 3$$

where $\xi(x) = (a-x)(b-x)$, we note that the first derivative of the modified Sinc basis function of $\xi(x)S_k(x)$ is defined at endpoints a and b and is equal to zero. Moreover, the functions $w_a(x)$ and $w_b(x)$ satisfy in the following boundary conditions

$$w_a(a) = w_b(b) = 1, w'_a(a) = w'_b(b) = 0, w_a(b) = w_b(a) = 0, w'_a(b) = w'_b(a) = 0,$$

and are obtained by Hermite interpolation as

$$w_a(x) = \frac{(2x + b - 3a)(b - x)^2}{(b - a)^3}, \quad w_b(x) = \frac{(-2x + 3b - a)(x - a)^2}{(b - a)^3}.$$

The $4N + 6$ unknown coefficients c_k and ρ_k in relation (3.4) are determined by substituting $\hat{u}_m(x)$ and $\hat{v}_m(x)$ into (3.2) and evaluating the result at the Sinc points (2.3).

Setting

$$\frac{d^i}{d\phi^i}[S_k(x)] = S_k^{(i)}(x), \quad 0 \leq i \leq 2, \quad (3.5)$$

and noting that

$$\frac{d}{dx}[S_k(x)] = S_k^{(1)}(x)\phi'(x), \quad (3.6)$$

$$\frac{d^2}{dx^2}[S_k(x)] = S_k^{(2)}(x)[\phi'(x)]^2 + S_k^{(1)}(x)\phi''(x), \quad (3.7)$$

and

$$\delta_{kj}^{(l)} = h^l \frac{d^l}{d\phi^l}[S_k(x)]_{x=x_j}. \quad (3.8)$$

By given approximations in (3.4) and using (3.5-3.7), we have

$$\hat{u}'_m(x) = c_{-N-1}w'_a(x) + \sum_{k=-N}^N c_k [\xi'(x)S_k(x) + \xi(x)\phi'(x)S_k^{(1)}(x)] + c_{N+1}w'_b(x), \quad (3.9)$$

$$\hat{v}'_m(x) = \rho_{-N-1}w'_a(x) + \sum_{k=-N}^N \rho_k [\xi'(x)S_k(x) + \xi(x)\phi'(x)S_k^{(1)}(x)] + \rho_{N+1}w'_b(x), \quad (3.10)$$

$$\begin{aligned} \hat{u}''_m(x) &= c_{-N-1}w''_a(x) + \sum_{k=-N}^N c_k \left[\xi''(x)S_k(x) + 2\xi'(x)\phi'(x)S_k^{(1)}(x) \right. \\ &\quad \left. + \xi(x)\phi''(x)S_k^{(1)}(x) + \xi(x)(\phi'(x))^2S_k^{(2)}(x) \right] + c_{N+1}w''_b(x), \end{aligned} \quad (3.11)$$

$$\begin{aligned} \hat{v}''_m(x) &= \rho_{-N-1}w''_a(x) + \sum_{k=-N}^N \rho_k \left[\xi''(x)S_k(x) + 2\xi'(x)\phi'(x)S_k^{(1)}(x) \right. \\ &\quad \left. + \xi(x)\phi''(x)S_k^{(1)}(x) + \xi(x)(\phi'(x))^2S_k^{(2)}(x) \right] + \rho_{N+1}w''_b(x). \end{aligned} \quad (3.12)$$

Now by substituting each terms of (3.2) with given approximations in (3.4), (3.11) and (3.12) and evaluating the result at the Sinc points x_j , we can obtain the

discrete Sinc-collocation system of nonlinear equations to determining the unknown coefficients $\{c_k\}_{k=-N-1}^{N+1}$ and $\{\rho_k\}_{k=-N-1}^{N+1}$ as

$$\left\{ \begin{array}{l} d_u \left\{ c_{-N-1} w_a''(x_j) + \sum_{k=-N}^N c_k \left[\xi''(x_j) S_k(x_j) + 2\xi'(x_j) \phi'(x_j) S_k^{(1)}(x_j) + \right. \right. \\ \left. \left. \xi(x_j) \phi''(x_j) S_k^{(1)}(x_j) + \xi(x_j) (\phi'(x_j))^2 S_k^{(2)}(x_j) \right] + c_{N+1} w_b''(x_j) \right\} + f \left(c_{-N-1} w_a(x_j) + \sum_{k=-N}^N c_k \xi(x_j) S_k(x_j) + c_{N+1} w_b(x_j), \rho_{-N-1} w_a(x_j) + \right. \\ \left. \sum_{k=-N}^N \rho_k \xi(x_j) S_k(x_j) + \rho_{N+1} w_b(x_j) \right) - \frac{1}{\Delta t} \left(c_{-N-1} w_a(x_j) + \sum_{k=-N}^N c_k \xi(x_j) S_k(x_j) + c_{N+1} w_b(x_j) \right) = -\frac{u^n}{\Delta t}, \\ \\ d_v \left\{ \rho_{-N-1} w_a''(x_j) + \sum_{k=-N}^N \rho_k \left[\xi''(x_j) S_k(x_j) + 2\xi'(x_j) \phi'(x_j) S_k^{(1)}(x_j) + \right. \right. \\ \left. \left. \xi(x_j) \phi''(x_j) S_k^{(1)}(x_j) + \xi(x_j) (\phi'(x_j))^2 S_k^{(2)}(x_j) \right] + \rho_{N+1} w_b''(x_j) \right\} + \\ g \left(c_{-N-1} w_a(x_j) + \sum_{k=-N}^N c_k \xi(x_j) S_k(x_j) + c_{N+1} w_b(x_j), \rho_{-N-1} w_a(x_j) + \sum_{k=-N}^N \rho_k \xi(x_j) S_k(x_j) + \rho_{N+1} w_b(x_j) \right) - \frac{1}{\Delta t} \left(\rho_{-N-1} w_a(x_j) + \right. \\ \left. \sum_{k=-N}^N \rho_k \xi(x_j) S_k(x_j) + \rho_{N+1} w_b(x_j) \right) = -\frac{v^n}{\Delta t}, \\ \\ j = -N-1, -N+1, \dots, N+1. \end{array} \right. \quad (3.13)$$

Also, we set

$$\xi^{(i)}(x_j) = \xi_j^{(i)}, \quad \phi^{(i)}(x_j) = \phi_j^{(i)}, \quad w_a^{(i)}(x_j) = w_{aj}^{(i)}, \quad w_b^{(i)}(x_j) = w_{bj}^{(i)}, \quad i = 0, 1, 2.$$

Using above relations and (3.8), system of equations (3.13) can be represented as

$$\left\{ \begin{array}{l} d_u \left\{ c_{-N-1} w_{aj}'' + \sum_{k=-N}^N c_k \left[\xi_j'' \delta_{kj}^{(0)} + \frac{2}{h} \xi_j' \phi_j' \delta_{kj}^{(1)} + \frac{1}{h} \xi_j \phi_j'' \delta_{kj}^{(1)} + \right. \right. \\ \left. \left. \frac{1}{h^2} \xi_j (\phi_j')^2 \delta_{kj}^{(2)} \right] + c_{N+1} w_{bj}'' \right\} + f \left(c_{-N-1} w_{aj} + \sum_{k=-N}^N c_k \xi_j \delta_{kj}^{(0)} + \right. \\ \left. c_{N+1} w_{bj}, \rho_{-N-1} w_{aj} + \sum_{k=-N}^N \rho_k \xi_j \delta_{kj}^{(0)} + \rho_{N+1} w_{bj} \right) - \\ \frac{1}{\Delta t} \left(c_{-N-1} w_{aj} + \sum_{k=-N}^N c_k \xi_j \delta_{kj}^{(0)} + c_{N+1} w_{bj} \right) = -\frac{u^n}{\Delta t}, \\ \\ d_v \left\{ \rho_{-N-1} w_{aj}'' + \sum_{k=-N}^N \rho_k \left[\xi_j'' \delta_{kj}^{(0)} + \frac{2}{h} \xi_j' \phi_j' \delta_{kj}^{(1)} + \frac{1}{h} \xi_j \phi_j'' \delta_{kj}^{(1)} + \right. \right. \\ \left. \left. \frac{1}{h^2} \xi_j (\phi_j')^2 \delta_{kj}^{(2)} \right] + \rho_{N+1} w_{bj}'' \right\} + g \left(c_{-N-1} w_{aj} + \sum_{k=-N}^N c_k \xi_j \delta_{kj}^{(0)} + \right. \\ \left. c_{N+1} w_{bj}, \rho_{-N-1} w_{aj} + \sum_{k=-N}^N \rho_k \xi_j \delta_{kj}^{(0)} + \rho_{N+1} w_{bj} \right) - \\ \frac{1}{\Delta t} \left(\rho_{-N-1} w_{aj} + \sum_{k=-N}^N \rho_k \xi_j \delta_{kj}^{(0)} + \rho_{N+1} w_{bj} \right) = -\frac{v^n}{\Delta t}, \\ \\ j = -N-1, -N+1, \dots, N+1. \end{array} \right. \quad (3.14)$$

To obtain a matrix representation of the equations (3.14). We define the $m \times m$

diagonal matrix as follow:

$$\mathbf{D}(s(x)) = \begin{pmatrix} s(x_{-N-1}) & 0 & 0 & \dots & 0 \\ 0 & s(x_{-N}) & 0 & \dots & 0 \\ \vdots & & \ddots & & \vdots \\ 0 & \dots & 0 & & s(x_{N+1}) \end{pmatrix}.$$

By using the above definitions and notations in (2.10), the system (3.14) can be represented by the following form:

$$\begin{cases} d_u[\mathbf{w}_a'', \mathbf{A}, \mathbf{w}_a'']\mathbf{c} + f([\mathbf{w}_a, \mathbf{B}, \mathbf{w}_b]\mathbf{c}, [\mathbf{w}_a, \mathbf{B}, \mathbf{w}_b]\mathbf{d}) - \frac{1}{\Delta t}[\mathbf{w}_a, \mathbf{B}, \mathbf{w}_b]\mathbf{c} = -\frac{\mathbf{u}^n}{\Delta t}, \\ d_v[\mathbf{w}_a'', \mathbf{A}, \mathbf{w}_a'']\mathbf{d} + g([\mathbf{w}_a, \mathbf{B}, \mathbf{w}_b]\mathbf{c}, [\mathbf{w}_a, \mathbf{B}, \mathbf{w}_b]\mathbf{d}) - \frac{1}{\Delta t}[\mathbf{w}_a, \mathbf{B}, \mathbf{w}_b]\mathbf{d} = -\frac{\mathbf{v}^n}{\Delta t} \end{cases} \quad (3.15)$$

where \mathbf{A} and \mathbf{B} are $(2N+3) \times (2N+1)$ matrices and $\mathbf{c}, \mathbf{d}, \mathbf{w}_a'', \mathbf{w}_b'', \mathbf{w}_a$ and \mathbf{w}_b are m -vectors as:

$$\mathbf{A} = \frac{1}{h^2}\mathbf{D}(\xi(\phi')^2)\mathbf{I}^{(2)} + \frac{1}{h}\mathbf{D}(2\xi'\phi' + \xi\phi'')\mathbf{I}^{(1)} + \mathbf{D}(\xi'')\mathbf{I}^{(0)}, \quad \mathbf{B} = \mathbf{D}(\xi)\mathbf{I}^{(0)}$$

$$\mathbf{w}_a = \begin{pmatrix} w_a(x_{-N-1}) \\ w_a(x_{-N}) \\ \vdots \\ w_a(x_{N+1}) \end{pmatrix}, \quad \mathbf{w}_b = \begin{pmatrix} w_b(x_{-N-1}) \\ w_b(x_{-N}) \\ \vdots \\ w_b(x_{N+1}) \end{pmatrix}, \quad \mathbf{c} = \begin{pmatrix} c_{-N-1} \\ c_{-N} \\ \vdots \\ c_{N+1} \end{pmatrix},$$

$$\mathbf{d} = \begin{pmatrix} \rho_{-N-1} \\ \rho_{-N} \\ \vdots \\ \rho_{N+1} \end{pmatrix}, \quad \mathbf{w}_a'' = \begin{pmatrix} w_a''(x_{-N-1}) \\ w_a''(x_{-N}) \\ \vdots \\ w_a''(x_{N+1}) \end{pmatrix}, \quad \mathbf{w}_b'' = \begin{pmatrix} w_b''(x_{-N-1}) \\ w_b''(x_{-N}) \\ \vdots \\ w_b''(x_{N+1}) \end{pmatrix},$$

also, the matrices $\mathbf{I}^{(0)}, \mathbf{I}^{(1)}$ and $\mathbf{I}^{(2)}$ are $(2N+3) \times (2N+1)$ and defined in (2.10). we rewrite the system (3.15) as following form

$$\begin{pmatrix} \mathbf{A}_u & \mathbf{0} \\ \mathbf{0} & \mathbf{A}_v \end{pmatrix} \begin{pmatrix} \mathbf{c} \\ \mathbf{d} \end{pmatrix} + \begin{pmatrix} f(\mathbf{M}\mathbf{c}, \mathbf{M}\mathbf{d}) \\ g(\mathbf{M}\mathbf{c}, \mathbf{M}\mathbf{d}) \end{pmatrix} = -\frac{1}{\Delta t} \begin{pmatrix} \mathbf{u}^n \\ \mathbf{v}^n \end{pmatrix}, \quad (3.16)$$

where

$$\mathbf{A}_u = d_u[\mathbf{w}_a'', \mathbf{A}, \mathbf{w}_a''], \quad \mathbf{A}_v = d_v[\mathbf{w}_a'', \mathbf{A}, \mathbf{w}_a''], \quad \mathbf{M} = [\mathbf{w}_a, \mathbf{B}, \mathbf{w}_b].$$

The system (3.16) is a nonlinear system of equations which consists of $4N + 6$ equations and $4N + 6$ unknowns. By solving this system by means of Newton's method, we can obtain approximate solutions $u_m(x)$ and $v_m(x)$ of (3.2) from (3.4). Of course with initial guess zero and fix point algorithm we can obtain a starting value for Newton's method.

4. Numerical results

In this section, by applying the Sinc collocation method on (1.1) to three test problems verify the analytical results discussed in the previous sections. In all of the examples considered in this paper, we choose $\alpha = 1$ and $d = \frac{\pi}{2}$ which yield $h = \frac{\pi}{\sqrt{2N}}$, also the errors are reported on uniform grids

$$U = \{z_0, z_1, \dots, z_k\}, \quad z_s = \frac{s}{k}, \quad s = 0, 1, \dots, k. \quad (4.1)$$

Example 1. We consider a predator-prey model with Beddington-DeAngelis functional response as following form

$$\begin{cases} \frac{\partial u}{\partial t} = d_u \frac{\partial^2 u}{\partial x^2} + u(\delta - u) - \frac{\beta uv}{1+pu+qv}, \\ \frac{\partial v}{\partial t} = d_v \frac{\partial^2 v}{\partial x^2} + v(1 - \frac{v}{u}), \end{cases} \quad (x, t) \in (0, 2\pi) \times (0, \infty) \quad (4.2)$$

subject to the homogeneous Neumann boundary condition

$$\frac{\partial u}{\partial x}(0, t) = \frac{\partial u}{\partial x}(2\pi, t) = \frac{\partial v}{\partial x}(0, t) = \frac{\partial v}{\partial x}(2\pi, t) = 0, \quad t \in (0, \infty).$$

All parameters appearing in model (4.2) are assumed to be positive constants. For this example, a unique positive equilibrium point (coexistence of predator and prey) has been derived as

$$u_s = v_s = \frac{r\delta - 1 - \beta + \sqrt{(1 + \beta - r\delta)^2 + 4r\delta}}{2r}, \quad r = p + q.$$

The qualitative analysis for this example is discussed in [14]. Here, we represent numerical simulations by Sinc-collocation method for various values of parameters in (4.2). Figures 1 and 2 display numerical simulations of example 1 for fixed values of parameters $N = 32, p = 0.6, q = 0.4, \beta = 12, d_v = 22, \Delta t = 0.01$ and for various values of δ and d_u . The example has been solved at final time $t = 30$. These parameters are taken from the literature [14]. In figure 1 we choose $\delta = 6$ such that the conditions of Theorem 1(2)(i) in [14] are satisfied. Then, by Theorem 1(2)(i) in [14], we know that (u_s, v_s) is locally asymptotically stable. In figure 2 we choose $\delta = 10$ such that the conditions of Theorem 1(3) in [14] are satisfied. Then, by Theorem 1(3) in [14], we know that (u_s, v_s) is unstable and non constant steady states appear.

The exact solution to this problem is unknown. So the accuracy of its numerical

solution will be computed using double mesh principle, therefore for each δ the maximum point wise errors are estimated as

$$E_{i,\delta}^m = \max_s |\hat{u}_i^m(z_s) - \hat{u}_i^{2m}(z_s)|, \quad i = 1, 2, \quad (4.3)$$

where $\hat{u}_1^m = \hat{u}_m(x)$, $\hat{u}_2^m = \hat{v}_m(x)$ are the approximation solutions of (3.4) for number of m Sinc points. let

$$E_\delta^m = \max_i E_{i,\delta}^m, \quad i = 1, 2. \quad (4.4)$$

Table 1 represent values of E_δ^m for various values of δ and N also for fixed values of $\beta = 12$, $d_u = 0.8$, $d_v = 22$, $p = 0.6$, $q = 0.4$, $\Delta t = 0.01$ and $t = 30$. These results show that the errors decrease with increasing N .

Table 1: Errors of E_δ^m for example 1 with $\beta = 12$, $d_u = 0.8$, $d_v = 22$, $p = 0.6$, $q = 0.4$, $\Delta t = 0.01$ and $t = 30$

$\delta \rightarrow$ $N \downarrow$	6	10	18
8	2.4×10^{-2}	3.79×10^{-2}	1.99×10^{-1}
16	2.91×10^{-3}	6.50×10^{-3}	2.10×10^{-2}
32	6.71×10^{-4}	6.13×10^{-4}	6.14×10^{-3}
64	1.68×10^{-4}	1.73×10^{-4}	5.40×10^{-4}

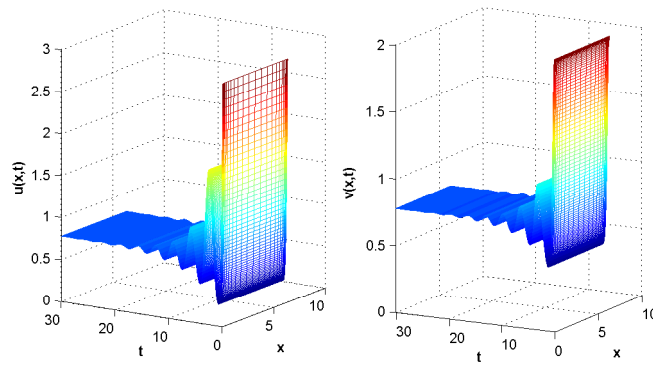


Figure 1: Numerical solutions of example 1 for values of $\delta = 6$, $p = 0.6$, $q = 0.4$, $\beta = 12$, $d_u = 0.8$, $d_v = 22$, with $\Delta t = 0.01$ at $t = 30$ and initial conditions $(u_0, v_0) = (3, 2)$ also $u_s = v_s = 0.7720$.

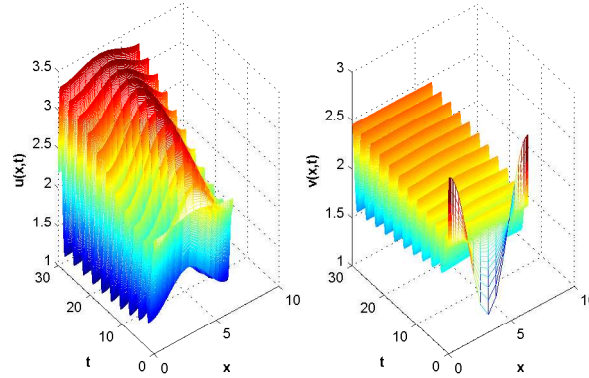


Figure 2: Numerical solutions of example 1 for values of $\delta = 10, p = 0.6, q = 0.4, \beta = 12, d_u = 0.8, d_v = 22$, with $\Delta t = 0.01$ at $t = 30$ and initial conditions $(u_0, v_0) = (2.5 + 0.001 \cos(\frac{x}{2}), 2 + 0.001 \cos(x))$ also $u_s = v_s = 2$.

Example 2. Second problem is given by

$$\begin{cases} \frac{\partial u}{\partial t} = d_u \frac{\partial^2 u}{\partial x^2} + u(1 - u) - \frac{\sqrt{uv}}{1 + \lambda \sqrt{u}}, \\ \frac{\partial v}{\partial t} = d_v \frac{\partial^2 v}{\partial x^2} + \beta v \left(-\frac{\gamma + \delta v}{1 + v} + \frac{\sqrt{u}}{1 + \lambda \sqrt{u}} \right), \end{cases} \quad (x, t) \in (0, \pi) \times (0, \infty) \tag{4.5}$$

with Neumann boundary conditions and initial conditions

$$u_x(0, t) = v_x(0, t) = u_x(\pi, t) = v_x(\pi, t) = 0, \quad u(x, 0) = u_0, v(x, 0) = v_0.$$

The system (4.5) is a spatial model exhibiting herd behavior in terms of square root of prey population and hyperbolic mortality $\frac{\gamma + \delta v}{1 + v}$ of predator.

Existence and uniqueness of positive equilibrium for this model have been proved in [31] analytically. Here, we present some numerical simulations by Sinc procedure, also, the example has been solved at final time $t = 2000, 1000$ and $t = 500$.

Fix $\delta = 0.5, \gamma = 0.2, \lambda = 1.5, d_u = 0.01, d_v = 0.8$. According to Theorem 3.1 of [31], the positive equilibrium (u_s, v_s) is asymptotically stable for $\beta > \beta_0 \approx 0.28$ and unstable for $\beta < \beta_0$. So, the system (4.5) undergoes a Hopf bifurcation at the bifurcation value $\beta = \beta_0$. The figures 3 and 4 verify the results of Theorem 3.1 in [31].

Moreover, for the parameter values $\delta = 0.5, \gamma = 0.2, \lambda = 1.5, d_u = 0.01, d_v = 5$ and $\beta = 4$, there exists a stable spatially inhomogeneous steady states. So, the system (4.5) undergoes a pitchfork bifurcation. The figure 5 verify the results of Theorem 3.1 in [31].

As the exact solution $u(x, t)$ and $v(x, t)$ of (4.5) are unknown, therefore the errors are estimated as (4.3) and (4.4) in example 1. Table 2 displays the results for this example for various values of N and β .

Table 2: Errors of E_β^m for example 2 with $\lambda = 1.5, \gamma = 0.2, \delta = 0.5, d_u = 0.01, d_v = 0.8, \Delta t = 0.01$ and $t = 100$

$\beta \rightarrow$	0.28	0.32	1.5
$N \downarrow$			
8	1.17×10^{-2}	1.15×10^{-2}	1.19×10^{-2}
16	2.30×10^{-3}	3.50×10^{-3}	1.15×10^{-3}
32	9.00×10^{-4}	8.84×10^{-4}	9.14×10^{-4}
64	2.08×10^{-4}	1.23×10^{-4}	4.10×10^{-4}

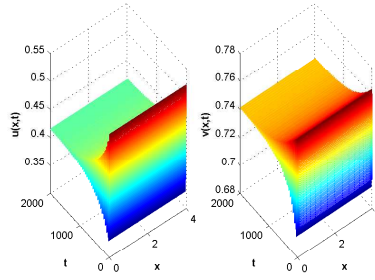


Figure 3: The positive equilibrium $(u_s, v_s) = (0.4153, 0.7410)$ of system (4.5) is asymptotically stable. Here we set $\delta = 0.5, \beta = 0.32, \gamma = 0.2, \lambda = 1.5, d_u = 0.01, d_v = 0.8$, and $N = 32$ with $\Delta t = 0.1$ at $t = 2000$ and initial conditions $(u_0, v_0) = (u_s + 0.02, v_s + 0.02)$.

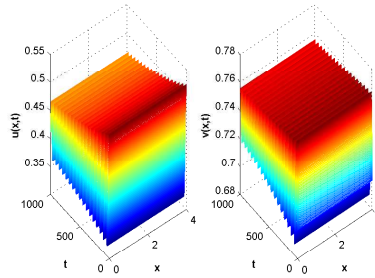


Figure 4: Numerical simulation of spatially homogeneous stable periodic solution bifurcating from the unstable equilibrium $(u_s, v_s) = (0.4153, 0.7410)$ of system (4.5). Here we set $\delta = 0.5, \beta = 0.28, \gamma = 0.2, \lambda = 1.5, d_u = 0.01, d_v = 0.8$, and $N = 32$ with $\Delta t = 0.1$ at $t = 1000$ and initial conditions $(u_0, v_0) = (u_s + 0.02, v_s + 0.02)$.

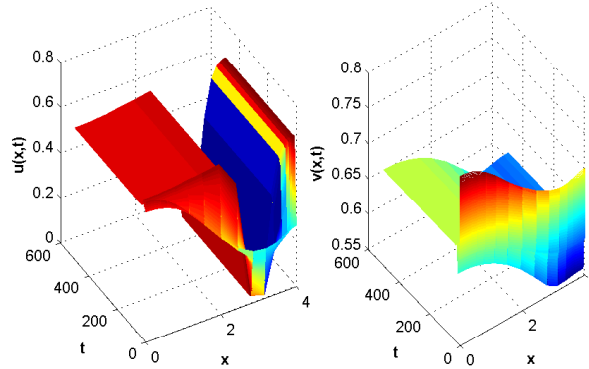


Figure 5: Numerical simulation of pitchfork bifurcation of positive constant equilibrium of system (4.5) for parameter values as $\delta = 0.5, \beta = 4, \gamma = 0.2, \lambda = 1.5, d_u = 0.01, d_v = 5$, and $N = 32$ with $\Delta t = 0.01$ at $t = 500$ and initial conditions $(u_0, v_0) = (u_s + 0.2 \cos(x), v_s + 0.05 \cos(x))$. The positive constant equilibrium $(u_s, v_s) = (0.4153, 0.7410)$ is unstable.

Example 3. We consider prey-predator reaction-diffusion system [32]

$$\begin{cases} \frac{\partial u}{\partial t} = d_u \frac{\partial^2 u}{\partial x^2} + Ru(1 - \frac{u}{K}) - \beta \frac{u^2 v}{1 + \lambda u^2}, \\ \frac{\partial v}{\partial t} = d_v \frac{\partial^2 v}{\partial x^2} + \gamma \frac{u^2 v}{1 + \lambda u^2} - \delta v, \end{cases} \quad (x, t) \in (-20, 20) \times (0, \infty) \quad (4.6)$$

subject to boundary conditions

$$u_x(-20, t) = v_x(-20, t) = u_x(20, t) = v_x(20, t) = 0,$$

and initial conditions

$$u(x, 0) = 1 - \frac{1}{2} \sin^{10}(\pi(x - 20)/40), \quad v(x, 0) = \frac{1}{4} \sin^{10}(\pi(x - 20)/40).$$

The growth rate of the prey $f(u) = Ru(1 - \frac{u}{K})$ is logistic and the predator's functional response $\frac{u^2 v}{1 + \lambda u^2}$ is Holling type III, the ratio γ/β and parameter R represent the maximal *per capita* predator and prey birth rates respectively, δ is the *per capita* predator death rate and K is the prey carrying capacity.

In the following, we adopt the parameters of system (4.6) according to the corresponding parameters in [32], our simulations confirm the results obtained in [32]. Figures present simulations of prey and predator for various cases of these parameters. In these figures the diffusion coefficient associated with the prey is much greater than the diffusion coefficient of the predators ($d_u = 1, d_v = 10^{-5}$). Figure 6(a) illustrates the prey-predator interaction characterized by the type III (sigmoid)

functional response, in which the rate of attack of the predator (v) accelerates at first and then decelerates towards satiation. Such sigmoid functional responses are typical of natural enemies which readily switch from one food species to another and/or which concentrate their feeding in areas where certain resources are most abundant. These are called prey-dependent responses because the feeding rate of consumers is dependent only on the density of prey.

This characteristic profile for the prey population density appears to be affected when we increase its carrying capacity K and the maximal *per capita* prey birth rate R (see figure 6(b)), or increase the prey carrying capacity K together with decreasing the *per capita* predator death rate δ (see figure 7). Also, according to (4.3) and (4.4), values of error for this example are given in table 3 for various values of N and K .

Table 3: Values of error for example 3 for various values of N and K with $\lambda = 10, \gamma = 0.001, \delta = 0.05, \beta = 1, R = 0.075, d_u = 1, d_v = 10^{-5}, \Delta t = 0.01$ and $t = 100$.

$K \rightarrow$ $N \downarrow$	1	5	10
8	5.21×10^{-1}	3.61×10^{-1}	8.27×10^{-2}
16	4.18×10^{-2}	2.18×10^{-2}	9.01×10^{-3}
32	6.51×10^{-3}	5.01×10^{-3}	7.81×10^{-4}
64	8.01×10^{-4}	6.12×10^{-4}	3.13×10^{-4}

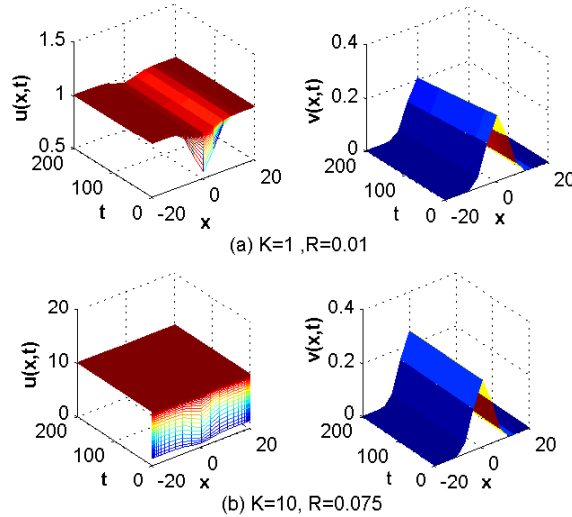


Figure 6: Comparative results on the densities of the prey $u(x, t)$ and predators $v(x, t)$ of example 3 for values of $d_u = 1, d_v = 10^{-5}, \delta = 0.01, \beta = 100, \gamma = 0.1, \lambda = 10$, and $N = 32$ with $\Delta t = 0.01$ at $t = 200$.

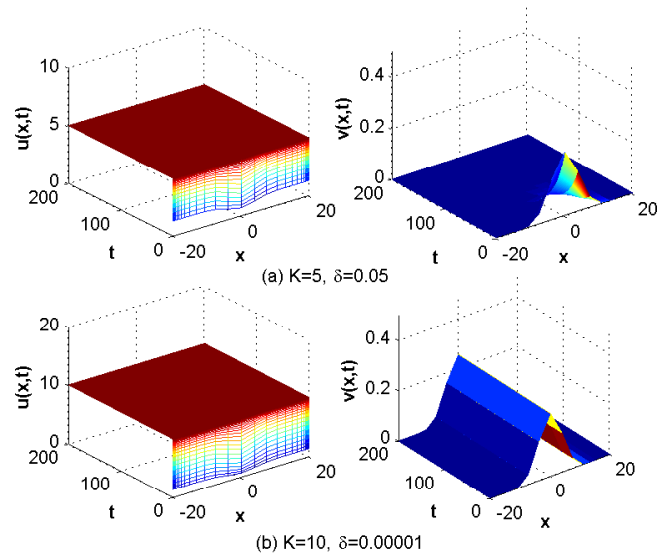


Figure 7: Comparative results on the densities of the prey $u(x,t)$ and predators $v(x,t)$ of example 3 for values of $d_u = 1$, $d_v = 10^{-5}$, $R = 0.075$, $\beta = 1$, $\gamma = 0.001$, $\lambda = 10$, and $N = 32$ with $\Delta t = 0.01$ at $t = 200$.

5. Conclusions

In this article, a numerical method was employed successfully for solving reaction-diffusion systems arising from two-species ecological models. This approach is based on the implicit Euler method for temporal discretization and the Sinc collocation method in the spatial direction. Results from numerical experiments indicate the efficiency and accuracy of proposed method. Also, from the figures 1-7 of numerical simulations, we get some useful information about the biological behaviors of species. Comparisons in given examples show the agreement of the approximate solutions with those presented in [14,31,32].

Acknowledgments

The authors are very grateful to the anonymous referees for their careful reading of this paper, and for providing helpful suggestions to improve this work.

References

1. Cantrell R., Cosner C., *Spatial ecology via reaction-diffusion equations*, Wiley series in mathematical and computational biology. Wiley ,Chichester (2003).
2. Holmes E., Lewis M., Banks J., Veit R., *Partial differential equations in ecology: spatial interactions and population dynamics*, Ecology, 75(1), 17-29, (1994).
3. Turing A. M., *The chemical basis of morphogenesis*, Phil. Trans.R. Soc.B, 237, 37-72, (1952),
4. Vande Koppel J., Crain C.M., *Scale-dependent inhibition drives regular tussock spacing in a fresh water marsh*, Am. Nat. ,168, 136-147,(2006).

5. Dufiet V., Boissonade J., *Dynamics of Turing pattern monolayers close to onset*, Phys. Rev. , 53,4883-4892,(1996).
6. Sun G.-Q., Zhang G., Jin Z., Li L., *Predator cannibalism can give rise to regular spatial pattern in a predator-prey system*, Nonlinear Dynam. , 58 75-84,(2009).
7. Sun G.Q., Jin Z., Li L., Li B.L., *Self-organized wave pattern in a predator-prey model*, Non-linear Dynam, , 60, 265-275,(2010).
8. Liu Q.X., Sun G.Q., Jin Z., Li B.L., *Emergence of spatiotemporal chaos arising from far-field break up of spiral waves in the plankton ecological systems*, Chin.Phys.B.,18, 506-515,(2009).
9. Wang W., Cai Y., Wu M., Wang K., Li Z. , *Complex dynamics of a reaction-diffusion epidemic model*, Nonlinear Anal. RWA, ,13, 2240-2258,(2012).
10. Baek H. , Jung DI., Wang Z., *Pattern formation in a semi-ratio-dependent predator-prey system with diffusion*, Discr Dyn Natur Soc. doi:10.1155/2013/657286,(2013).
11. Garvie M, *Finite-difference schemes for reaction-diffusion equations modeling predator-pray interactions in MATLAB*. Bullet MathBiol.,69, 931-56,(2007).
12. Mimura M. , Sakaguchi H., Matsushita M., *Reaction-diffusion modelling of bacterial colony patterns*, Physica A. , 282,283-303,(2000).
13. Petrovskii S. , Morozov AY., Venturino E., *Allee effect makes possible patchy invasion in a predator-prey system*, Ecol Lett , 5, 345-52,(2002).
14. Jiang H. , Wang L., Yao R., *Numerical simulation and qualitative analysis for a predator-prey model with B-D functional response*, Mathematics and Computers in Simulation , 117, 39-53,(2015).
15. Wang W., Liu QX., Jin Z., *Spatiotemporal complexity of a ratio-dependent predator-prey system*. Phys Rev E. , 75, 1539-3755,(2007).
16. Garvie M., Trenchea C., *Spatiotemporal dynamics of two generic predator-prey models*. J Biol Dyn.,4, 559-570,(2010).
17. Kolade M. Owolabi, Kailash C. Patidar, *Higher-order time-stepping methods for time-dependent reaction-diffusion equations arising in biology*, Applied Mathematics and Computation, 240, 30-50,(2014).
18. Shakeri F., Dehghan M., *The finite volume spectral element method to solve Turing models in the biological pattern formation*, Computers and Mathematics with Applications, 62, 4322-4336,(2011).
19. Marcus R. Garvie , Philip K. Maini , Catalin Trenchea, *An efficient and robust numerical algorithm for estimating parameters in Turing systems*, Journal of Computational Physics , 229 (19),7058-7071,(2010).
20. Kolade M.Owolabi and Kailash C. Patidar, *Numerical simulations of multicomponent ecological models with adaptive methods*, Theoretical Biology and Medical Modeling , DOI10.1186/s12976-016-0027-4, (2016).
21. Marcus R. Garvie , Burkardt J., Morgan J., *Simple Finite Element Methods for Approximating Predator-Prey Dynamics in Two Dimensions Using Matlab*, Bull Math Biol, 77,548-578,(2015).
22. Stenger F., *A Sinc Galerkin method of solution of boundary value problems*, Math. Comp. , 33, 35-109,(1979).
23. Lund J., Bowers K., *Sinc Methods for Quadrature and Differential Equations*, SIAM, Philadelphia, PA,(1992).
24. Stenger F., *Numerical Methods Based on Sinc and Analytic Functions*. Springer, New York,(1993).
25. Bialecki B. , *Sinc-collocation methods for two-point boundary value problems*. IMA J. Numer. Anal.,11, 357-375,(1991).

26. Rashidinia J. , Nabati M., Barati A., *Sinc-Galerkin method for solving nonlinear weakly singular two point boundary value problems*, International Journal of Computer Mathematics, , DOI: 10.1080/00207160.2015.1085027,(2015).
27. Rashidinia J. , Barati A., Nabati M., *Application of Sinc-Galerkin method to singularly perturbed parabolic convection-diffusion problems*, Numer. Algor. , 66,643-662,(2014).
28. EL-GAMEL M., *The sinc-Galerkin method for solving singularly-perturbed reaction-diffusion problems*, Electronic Transactions on Numerical Analysis. , 23, 129-140,(2006).
29. Okayama T., Matsuo T., Sugihara M., *Sinc-collocation methods for weakly singular Fredholm integral equations of the second kind*, Journal of Computational and Applied Mathematics., 234, 1211-1227,(2010).
30. Saadatmandi A., Dehghan M., *The use of Sinc-collocation method for solving multi-point boundary value problems*, Commun Nonlinear Sci Numer Simulat , 17(2), 593-601,(2012).
31. Tanga X., Song Y.,*Bifurcation analysis and Turing instability in a diffusive predator-prey model with herd behavior and hyperbolic mortality* ,Chaos, Solitons and Fractals , 81, 303-314,(2015).
32. Narcisa A., Dimitriu G., *On a prey-predator reaction-diffusion system with Holling type III functional response*, Journal of computational and applied mathematics , 235(2), 366-379,(2010).

Ali Barati,
Islamabad Gharb Faculty of Engineering
Razi University, Kermanshah
Iran.
E-mail address: alibarati@razi.ac.ir

and

Ali Atabaigi,
Department of Mathematics, Faculty of Science
Razi University, Kermanshah
Iran.
E-mail address: a.atabeigi@razi.ac.ir